"Gheorghe Asachi" Technical University of Iasi, Romania

ASSESSMENT OF PHOTOGRAMMETRIC MAPPING TO DETERMINE THE VOLUME OF CONSTRUCTION AND DEMOLITION WASTE

Juan Antonio Araiza-Aguilar[1*], María Neftalí Rojas-Valencia[2], Constantino Gutiérrez-Palacios[3], Hugo Alejandro Nájera-Aguilar[1], Rubén Fernando Gutiérrez-Hernández[4]

[1]School of Environmental Engineering, University of Science and Arts of Chiapas,
North beltway 1150, Lajas Maciel, 29039 Tuxtla Gutierrez, Chiapas, Mexico
[2]Institute of Engineering, National Autonomous University of Mexico, External circuit,
University City, 04510 Coyoacan borough, Mexico City, Mexico
[3]Faculty of Engineering, National Autonomous University of Mexico, External circuit, University City,
04510 Coyoacan borough, Mexico City, Mexico
[4]Department of Chemical and Biochemical Engineering, National Technology of Mexico - Technological Institute
of Tapachula, Km 2, Highway to Puerto Madero, 30700, Tapachula, Chiapas, Mexico

Abstract

This paper evaluates the products generated by Unmanned Aerial Vehicles used as tools to survey objects on surfaces. A Digital Elevation Model obtained from a photogrammetric process is then compared with another model obtained from a traditional Total Station survey. Different precision metrics are used, both for the Digital Elevation Models generated and for the points collected. The results of both forms of surveying objects on surfaces show that the products obtained with the photogrammetric method deviate importantly from those obtained with the Total Station survey (overestimations in some points of up to 50 cm). However, because it results in significant time savings in data collection, the photogrammetric method is generally more useful. The precision values of the Digital Elevation Model produced by the photogrammetric method give a ground resolution of 4.79 cm/pix, a mean error of ground control points of 1.31 cm and a point density of 436 points/m^2. On the other hand, the comparative precision values between the products of both survey methods are 0.23 m in the Absolute Mean Deviation and 0.58 m in the Root of the Mean Square Deviation. Additionally, more precise metrics were also obtained by analyzing zones with different densities of collected points. It should be noted that the main differences between the products of both survey methods were due to the low density of sampling points within the study area, particularly in the case of Total Station survey.

Keywords: accuracy assessment, construction demolition waste, photogrammetry, UAV

1. Introduction

Construction and Demolition Wastes (CDWs) are materials generated in the demolition, remodeling and construction of public and private works. Materials discarded during virgin material extraction processes are also included (OGFD, 2015). CDWs are typically made up of inert materials such as concrete, brick, rock chips, ceramics, wood, plastics, and others (Contreras et al., 2016; Lau et al., 2008); but they also sometimes include hazardous materials such as asbestos and paint or solvent containers (Chen and Zhou, 2020; Yu et al., 2018). If CDWs are handled incorrectly, they can have undesirable effects such as changes in land use, contamination of surface and groundwater, dusts and negative aesthetic impacts (Chen et al., 2000; Gangolells et al., 2009; Zolfagharian et al., 2012).

Because of the large amounts of CDW generated daily, the heterogeneity of its composition

---

[*]Author to whom all correspondence should be addressed: e-mail: araiza0010@hotmail.com; Phone: +52 961 138 14 20

and the difficulty in identifying production sources, CDW quantification is a complex matter. Currently, various CDW quantification methods based on the extension of the analysis area (regional or local), on the way to quantify the volumes (direct and indirect) or on a combination of them are used (Wu et al., 2014). For example, in the studies by Bergsdal et al. (2007), Kleemann et al. (2016), McBean and Fortin (1993), NAUM (2017), Poon (1997) and Yost and Halstead (1996), the amounts of waste produced at the regional, state or national level are estimated, using indirect methods such as per-capita multipliers, area-based calculations or even remote perception with satellite images. Other papers, such as Kartam et al. (2004), Lau et al. (2008) and Poon et al. (2004), disclose local studies, which include direct measurements such as weighing the waste produced or measuring its volume on the site.

In order to determine CDW volumes on a site, methods for surveying objects on the surface are commonly used, such as the polar space method with Total Station (TS), the GNSS method, laser scanning and also photogrammetric methods (Blišťan and Kovanič, 2012). These methods differ in terms of their principles, precision, costs of instruments, equipment, software, and also in terms of the speed of measurement of the objects under study (Kovanič and Šimčák, 2014). As a result of the process of field measurements and post-processing of cabins data, a set of coordinates and altitudes (Coordinates X, Y, Z) of the points necessary for an analysis and evaluation of the object studied are obtained (Kršák et al., 2016).

Recently, the use of Unmanned Aerial Vehicles (UAVs) has become very popular, mainly due to the notable decrease in acquisition costs, increased operational benefits (flight time, ease of operation), and the improvement of the sensors used (cameras, gps, lidar, etc.) (Berie and Burud, 2018; Nex and Remondino, 2014; Otto et al., 2018). In the area of construction engineering, UAVs have been used to carry out surveys during the preparation phase of construction sites, to carry out monitoring during the construction phases, and to perform inspections in the post-construction stage (Li and Liu, 2018). UAVs have become a serious alternative for data collection, mapping with high spatio-temporal resolution, and they currently represent a low-cost alternative to traditional manned aerial photogrammetry (Haala et al., 2011).

Some products derived from a survey with UAVs are: i) point cloud, which are points positioned three-dimensionally in space, which store information related to the position, color and reflectivity of the surveyed object; ii) orthoimages or georeferenced mosaics, which result from joining several individual photographs taken by the UAV, but which have been corrected to represent an orthogonal projection without perspective effects; and iii) Digital Elevation Model (DEM), which corresponds to a model of the surface of the object, but based on cells or pixels, where each of them stores the position and height. It is important to mention that these products are generated in photogrammetric software through a process known as Structure from Motion (SfM), which builds three-dimensional structures from sequences of two-dimensional images.

The accuracies achieved by UAV surveys are variable, because they depend on multiple factors such as flight planning, camera quality and calibration, the georeferencing strategy, the technical characteristics of the equipment, the number of control points and others (Sanz et al., 2018). As a result, X, Y, and Z accuracies ranging from a few millimeters to tens of millimeters are obtained. For example, in Casella et al. (2020) and Uysal et al. (2015), almost flat surfaces such as beaches and small hills are surveyed, and vertical errors of 0.006 m and 0.06 m, respectively, are achieved. In Hugenholtz et al. (2013), Hugenholtz et al. (2015) and Sun et al. (2020), geomorphological land surveys are carried out for medium and large projects, with vertical errors ranging from 0.068 m to 0.29 m.

This paper evaluates the products generated by UAVs used as tools to survey objects on surfaces. A DEM obtained from a digital photogrammetric process with UAVs is then compared with another DEM obtained from a traditional TS survey. Different precision metrics are used, both for the DEM generated and for the points collected. This paper argues in favor of the use of UAVs to determine CDW volumes, since the other techniques are very complicated and expensive. The results offered in this paper will be useful for decision-making, for example, to implement more realistic policies in the environmental and construction engineering areas, to establish new waste disposal facilities, and to determine the number of CDW collection trucks needed in case of contingencies. It should also be noted that the methods employed in this work can be used in both small and large projects.

2. Material and methods

2.1. Description of the study area

The study area is located within a property called CEDEC, to the northwest of Mexico City, Mexico. This property is located at the coordinates UTM 2,153,058.92 N and 479,157.43 E (Zone 14 N, WGS84), it occupies a total area of 22,065 m^2 (Fig. 1). This property is currently used to temporarily store CDW generated by the Miguel Hidalgo borough, but in the future it will be used to establish a recycling plant for this type of waste. Some areas are clearly distinguishable, for example, administrative area, warehouse area, maneuvering yard, CDW storage area and external areas. The comparative analysis of the survey methodologies will be carried out only as regards the CDW storage area, which occupies an approximate area of 2,827 m^2.

2.2. Total station survey

The basic principle to determine the

coordinates of the points using TS is the measurement of horizontal and vertical angles and slopes or distances from TS to the point to be measured (Kovanič and Šimčák, 2014). Commonly this method is called spatial polar, and all the calculations it involves are computed inside the instrument. To carry out the survey inside the CEDEC property, a SOKKIA brand TS, model SET620K was used (Table 1). With this instrument, the most visible CDW mounds were surveyed, which allowed the digital recreation of the morphology of the terrain. In total, 761 points were collected (Fig. 2a), but some of them were removed to avoid errors in the computed metrics. It is important to mention that the surveys (with UAV and TS) were performed at different times so earthworks may have been carried out by workers or machinery between the surveys.

Table 1. SOKKIA SET620K technical data

Magnification / Resolving power	26 x / 3.5"
Accuracy H&V	6" / 1.9 mg on / 0.03 mil
Measuring range	>4,000 m
Accuracy with prism	Fine mode: (2 + 2 ppm x D) mm Rapid mode: (5 + 5 ppm x D) mm
Size	W 165 x D 173 x H 341 mm
Weight	5.1 kg

2.3. Photogrammetric survey with UAV

The photogrammetric survey with UAV also involves different stages.

i) Flight planning, which can be performed in the office or on site. In this stage, the parameters of the cameras mounted on the UAVs should be taken into account, such as focal length, sensor size, orientation and shutter speed; as well as the height and speed of the flight, the percentage of straight and side overlap between photos. Meteorological aspects such as precipitation, speed and direction of wind must also be considered. Some recommendations for different types of surveys with UAVs can be seen in Federman et al. (2017), Mouget and Lucet (2014), Rusnák et al. (2018) and Suziedelyte et al. (2016). Eqs. (1-4) are the most important of this phase.

$$E = 1 : e = \frac{f}{H} \tag{1}$$

$$GSD = \frac{pix \cdot H}{f} \tag{2}$$

$$NFL = \left(\frac{W}{SP} \right) + 1 \tag{3}$$

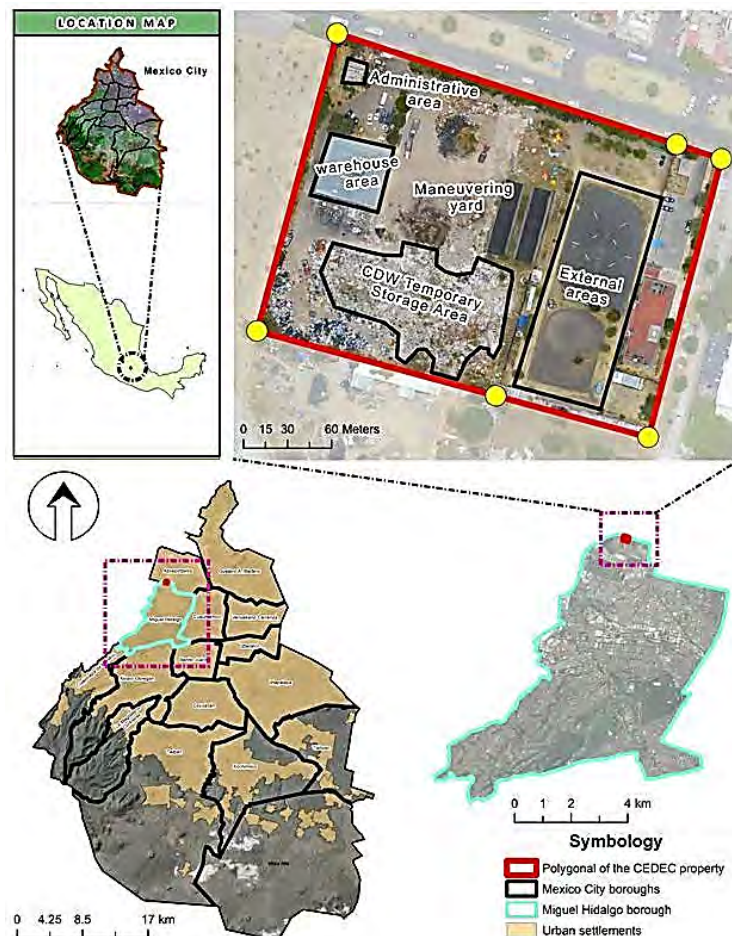$$SP = W_a \cdot \left(\frac{\% \, sidelap}{100} \right) \tag{4}.$$

Fig. 1. Study area

In these equations E is the scale of the photograph; e is the denominator of the image scale; f is the focal length of the camera lens; H is the height of the UAV flight; GSD is Ground Sample Distance or pixel size in the field; pix is the Linear dimension of the pixel; NFL is the number of flight lines; W is the width of the area to be mapped; SP is the distance between the flight lines; W_a is the ground cover that has an image; *% sidelap* is the percentage of overlap between images of adjacent flight lines. It should be noted that, in digital photogrammetry, all these equations can be automatically computed by specialized desktop or portable software.

ii) Acquisition of Ground Control Points (GCP), which must be carried out prior to the UAV flight, placing ground marks so that these points are captured by the photographs and subsequently serve to digitally align, scale and reconstruct the objects of interest (Federman et al., 2017). The equipment used can be a TS or a GNSS receiver using RTK (Real Time Kinematics) technique. Some recommendations on the number of GCPs and their distribution over the study area can be seen in Agüera et al. (2017) and Harwin and Lucieer (2012).

iii) Data processing, which is carried out within a robust computer with specialized software, such as pix4D, Agisoft Metashape and others. Through these softwares it is possible to orient the photographs taken by UAVs, create point clouds, meshes, textures, DEMs and orthomosaics.

In this work, the images were taken by a Professional Phantom 3 multirotor UAV, which has a 3-axis gimbal and a 12.4 megapixel 1/2.3" CMOS digital camera. Through this equipment, 62 photographs were captured and georeferenced with the UAV's internal GPS. The *NFL* was 5 to cover the entire study area. The flight was performed at a speed of 15 m/s, at a height of 105 m and with 70% overlap and sidelap. A GNSS receiver SOKKIA GRX2 kit was used to acquire GCPs randomly distributed throughout the study area. The recommendations of Agüera et al. (2017) were considered to obtain optimal precision results, therefore 15 GCPs were collected using the RTK technique with base station and rover (Fig. 2b-c). In addition, each GCP was adequately marked on the ground to georeference images in subsequent processes. The specifications of the GNSS receiver and UAV equipment are described in Table 2.
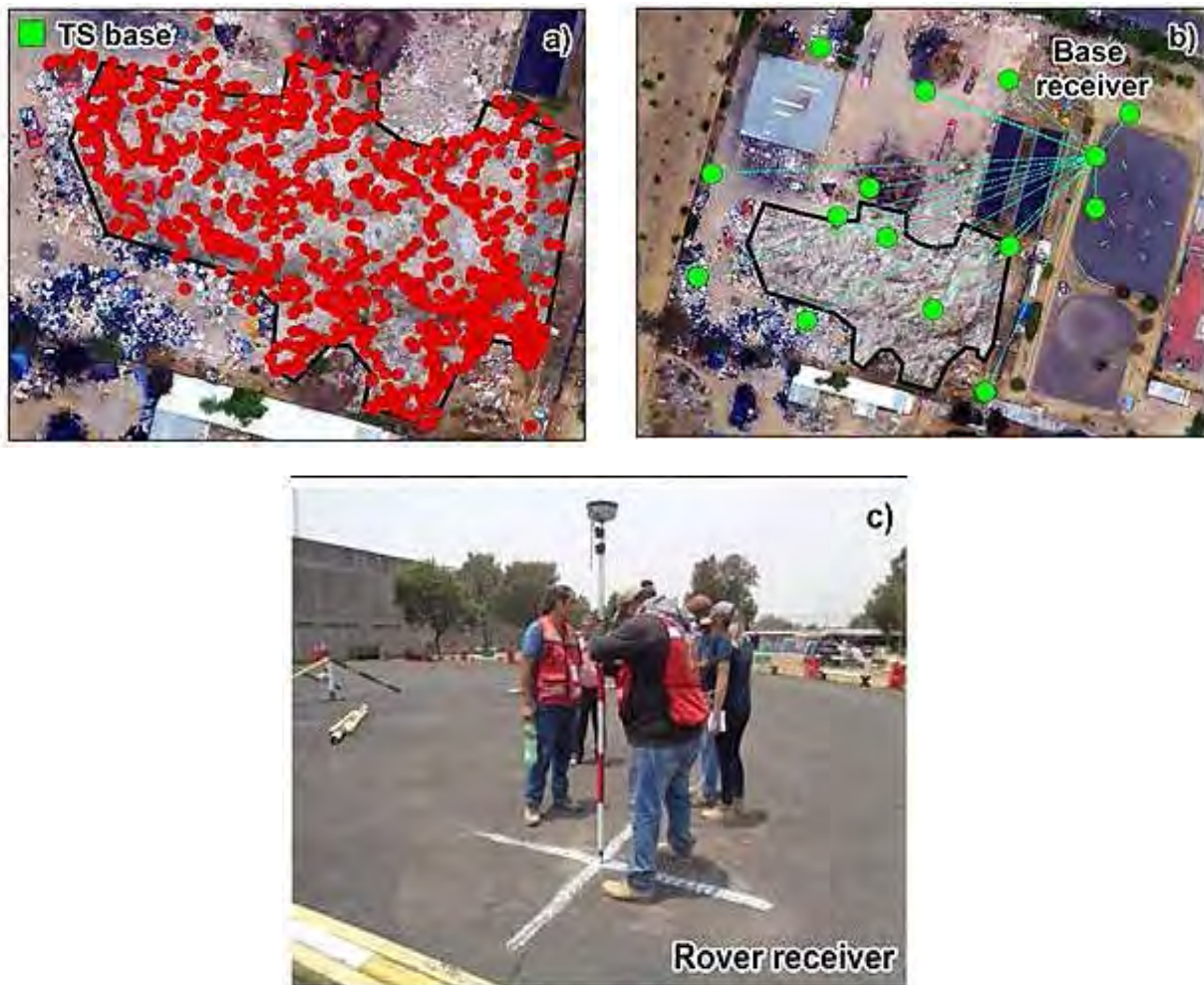

Fig. 2. Surveys with TS and GNSS receivers-UAV: a) distribution of points surveys with TS;
b) distribution of surveyed points with GNSS receivers and RTK technique; c) survey with rover GNSS receiver

Table 2. Technical specifications of the photogrammetric survey equipment

GNSS receiver SOKKIA GRX2	*Professional Phantom 3 multirotor*
226 Channels (GPS+Glonass+SBAS)	Manufacturer's Product Type: quadcopter
Positioning Accuracy: RTK (L1 + L2) H: 5 mm + 0.5 ppm, V: 10 mm + 0.8 ppm	Operating Frequency: 2.4 GHz
Update/output rate: 1 Hz, 5 Hz, 10 Hz, 20 Hz (10 Hz RTK Standard)	Max Operating Distance: 3 miles
Weight (GRX2 receiver / battery) 1.0 kg (2.20 lb.) / 195 g (6.9 oz.)	Sensor Resolution: 12.4 megapixels
Standard battery: Detachable, Li-ion battery, 7.2V, 5240 mAh	Supported Battery Configurations: 4S / lithium polymer / 4480 mAh

The images acquired by the UAV were captured in zenith format, and then incorporated into the Agisoft Metashape Professional edition software, version 1.5.5. The process began with image orientation and alignment, based on EXIF metadata and featured an image matching approach. The process continued with the construction of dense point clouds, geometries and textures to achieve a realistic appearance (Agüera et al., 2017).Quality and accuracy are important, but they depend on the power of the computer equipment. In this work, a high accuracy approach was used in photo alignment, while a medium quality procedure was used for the generation of dense point cloud.

In geomatics applications, it is necessary to georeferenced the data with the GCPs surveyed in the field. In this work the 15 GCPs collected were used. Finally, the orthoimage was exported and a DEM was generated from the point cloud. The results of the photogrammetric data processing within the software offer good precision characteristics. A ground resolution of 4.79 cm/pix was obtained. The average error of the GCP was 1.31 cm, which corresponds to 1.091 pix. In addition, a point density of 436 points/m^2 was obtained.

2.4. DEM construction

Representation of topographic relief shapes can be done through vector or raster models, for example, based on TIN (Triangulated Irregular Network) or cell matrices (pixels). In this paper, the CDW storage surface was modeled through the raster approach, because of its low requirements for processing a large amount of data. Furthermore, according to Kovanič and Šimčák, (2014), DEM planimetry coordinate information is calculated subsequently, and not stored directly in the computer memory during the computation process.

The DEM generated by the Agisoft Metashape software (Fig. 3a) was built from the point cloud

captured in the photographs, which means that the Inverse Distance weighted was used as an interpolation method in that software. The DEM generated by the points surveyed with TS was built through the Topo to Raster tool of the ArcGis 10.x software (Fig. 3b), which is an interpolation method specifically designed to create hydrologically correct DEM (ESRI, 2020). The tool interpolates elevation values to create a raster while imposing constraints that ensure a connected drainage structure, and correct representation of ridges and streams.

(a)
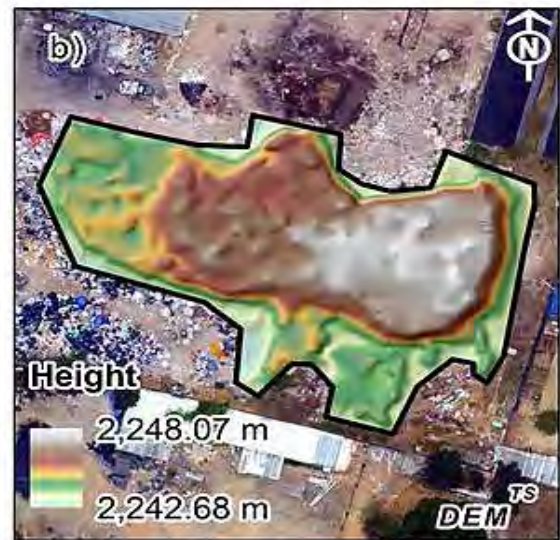
(b)

Fig. 3. DEM surfaces generated; a) DEM surface generated by Agisoft Metashape software; b) DEM surface generated by the Topo to Raster interpolator

In the works of Arseni et al. (2019), Bergonse and Reise (2015) and Habib et al. (2020), optimal results in the modeling of natural landscapes have been obtained with the Topo to Raster interpolator, results that are even better than those generated by the Inverse Distance weighted or kriging methods. This interpolator is versatile because it models the erosive

force produced by water in geoforms. In addition, it admits several types of natural features as input data (elevation points, contour lines, stream centerline, sink, boundary, lake, cliff, coast).

Obviously, each interpolation method used, standard or custom, will produce different results. However, in this work, the use of the Topo to Raster tool permits to model the geomorphology of the terrain as adequately as possible based on the data collected in the field.

It is important to mention that a third DEM was built to compare the volumes obtained with the above mentioned DEMs. Its base height was 2,242.63 m. Additionally, the reference system and spatial resolution of all DEMs were WGS84 UTM zone 15N and 5 cm, respectively.

2.5. Accuracy analysis between surveys

In this paper, different techniques were used to evaluate the accuracy between the surveys, which are mainly based on the analysis of points and DEM surfaces created. In order to assess the differences between the DEMs, spatial distribution maps of the deviations (*D*) were generated. Through a simple difference between the pixel values of both raster layers (*D = pix DEM^{UAV} – pix DEM^{TS}*), the places within the CDW storage area showing the greatest deviations were identified.

The Accuracy assessment between points was performed by comparing height values for several points surveyed by TS, with respect to the values extracted from the MDE generated by the Agisoft Metashape software. Eqs. (5-6) show the vertical accuracy measurements used. In these equations, MAD_Z is the Mean Absolute Deviation; $RMSD_Z$ is the Root of the Mean Square Deviation; Z_i^{TS} is the height at the i-th point measured with TS; Z_i^{DEM} is the height at the i-th point extracted from the DEM; finally, *n* is the number of points used in the analysis.

These measurements will express the mean deviation in the same unit of the variable. Furthermore, both metrics can vary from 0 to ∞ and are indifferent to the direction of the errors (underestimates and overestimates). They are negatively oriented metrics, which means that lower values are better because they represent smaller errors (Chow and Kar, 2017).

$$MAD_Z = \frac{1}{n}\sum_{i=1}^{n}\left|Z_i^{DEM} - Z_i^{TS}\right| \quad (5)$$

$$RMSD_Z = \sqrt{\frac{1}{n}\sum_{i=1}^{n}\left(Z_i^{DEM} - Z_i^{TS}\right)^2} \quad (6)$$

The coefficient of determination R^2 was also used, but as a metric to determine how significant the correlation between the compared points is.

Finally, the volumes generated by both DEMs, were compared with a third DEM. A visual analysis of 4 sections drawn along the length and width of the CDW storage area was carried out. As in Kršák et al.

(2016), in drawn sections, the differences between the curves of both surfaces were reviewed.

3. Results and discussion

3.1. Analysis of differences between DEM built and collected points

Fig. 4a- b shows the vertical deviation maps. It is observed that the smallest deviations are found in the central zone of the CDW storage area, with values ranging between 0 and ± 20 cm. The highest deviations are found in the extreme north and northeast, with values exceeding ± 50 cm in some specific sites. Fig. 4c-d summarizes the deviation information in terms of areas. It can be seen that a surface of 1,827.87 m^2, equivalent to 64.65% of the total area, is overestimated, that is, the value given by the DEM produced by the Agisoft Metashape software is higher than the DEM value generated by the points surveyed by TS.

The deviations found in this work are due to several systematic or accidental factors. First, the densities of points collected to build the DEM were different. The photogrammetric process with UAVs commonly offers values greater than 100 points/m^2 (Jiménez et al., 2017). In this work, values of 436 points/m^2 were obtained in the photogrammetric process, while the TS survey produced a density of 0.24 points/m^2. Note that, to obtain a greater number of points with the traditional methods, detailed surveys would have to be carried out for each m^2 of the study area, but there could also be distortions, since the survey method with TS is intrusive, which means that small mounds of CDW would be destroyed by walking over them to determine their height. With the use of UAVs, less intrusive actions are generated, because the presence of field devices is limited to the placement of ground targets and photographic shots from the air. Another factor of possible variability between the DEMs constructed is the interpolation methods used. It is well known that the vast majority of them can be used for general purposes, including modeling landscapes, but each method is dependent on various starting data, for example, number of elevation points or contour lines, pixel size or output spatial resolution, search radius for the points considered, etc.

Additionally, it is important to note that some methods produce exact surfaces while others generate approximate surfaces (Burrough and McDonnell, 1998). In this work, the interpolator used by Agisoft Metashape software is exact, which means there is no variation between the point values used in the interpolator and the values of the generated surface at that same location.

On the other hand, the Topo to Raster interpolator generates approximate surfaces but with the possibility of adding contour lines and other natural characteristics in order to produce a detailed DEM. In any case, due to the low number of points collected with TS, the DEM generated by the Agisoft

Metashape software seems to be more congruent with the geoforms present in the study area.

Finally, external or accidental factors such as the handling and composition of CDW also caused important deviations. CDWs that are stored on construction sites create small but complex topographies on the ground. For example, in the studies by Lau et al. (2008) and Wu et al. (2019), the most prevalent CDW materials are wood, metal and concrete, which commonly have flat and voluminous shapes. On the other hand, in the work of Cardoso et al. (2015), the wastes have already been separated and crushed, so the characteristics are similar to those of stone aggregates, and their topographies are less complex. In this work, the topographic forms found in the study area were complex, since the CDWs had not been crushed or separated. In this way, the UAV survey offered greater benefits in terms of time, costs, and quality compared to the TS survey.

Regarding the point analysis, initially 683 points collected by the TS were compared with values extracted from the DEM generated in the photogrammetric process. Values of $MAD_Z = 0.23$ m, $RMSD_Z = 0.58$ m and $R^2 = 0.80$ were obtained. These values would commonly indicate high accuracies, however, for surveying objects on surfaces they appear to be too high.

As a matter of fact, Casella et al. (2020) and Uysal et al. (2015) also compare surface surveys, obtaining $RMSD_Z$ values of 0.0662 m and 0.16 m, which are much lower than those obtained in this work, but with less abrupt surveyed surfaces.

In addition to the above, large deviations were found in 36 of the 683 points analyzed, which are located in the extreme north of the CDW storage area (Fig 5a). These points correspond to places where external factors may have created earthworks and therefore low metrics. After computing the precision metrics again, without considering the highly deviated values, more realistic results were obtained, $MAD_Z = 0.12$ m, and $RMSD_Z = 0.17$ m (Fig 5b).

By further detailing the analysis across zones with different numbers of collected points, zonal precision measurements can be obtained. Fig. 6a shows the study area classified into 3 zones that have different numbers of points surveyed with TS. The zone with the highest number of surveyed points occupies an area of only 125.70 m^2, and its density is 0.55 points/m^2 (Fig. 6b). The precision values obtained in these places are the highest, even approaching the values reported in other surveys of objects on surfaces ($MAD_Z = 0.09$ m, and $RMSD_Z = 0.12$ m). The zone with mean point density (0.28 points/m^2) occupies an area of 1,597 m^2, but its precision values decrease to $MAD_Z = 0.11$ m, and $RMSD_Z = 0.16$ m (Fig. 6c). In areas with low point density (0.11 points/m^2), the precision metrics decrease even more ($MAD_Z = 0.13$ m, and $RMSD_Z = 0.19$ m) (Fig. 6d). Note that Fig. 6b-6d show the coefficient of determination R^2, which gradually decreases as the point density also decreases. The above indicates that some points collected may have significant deviations, the product of systematic or accidental errors.
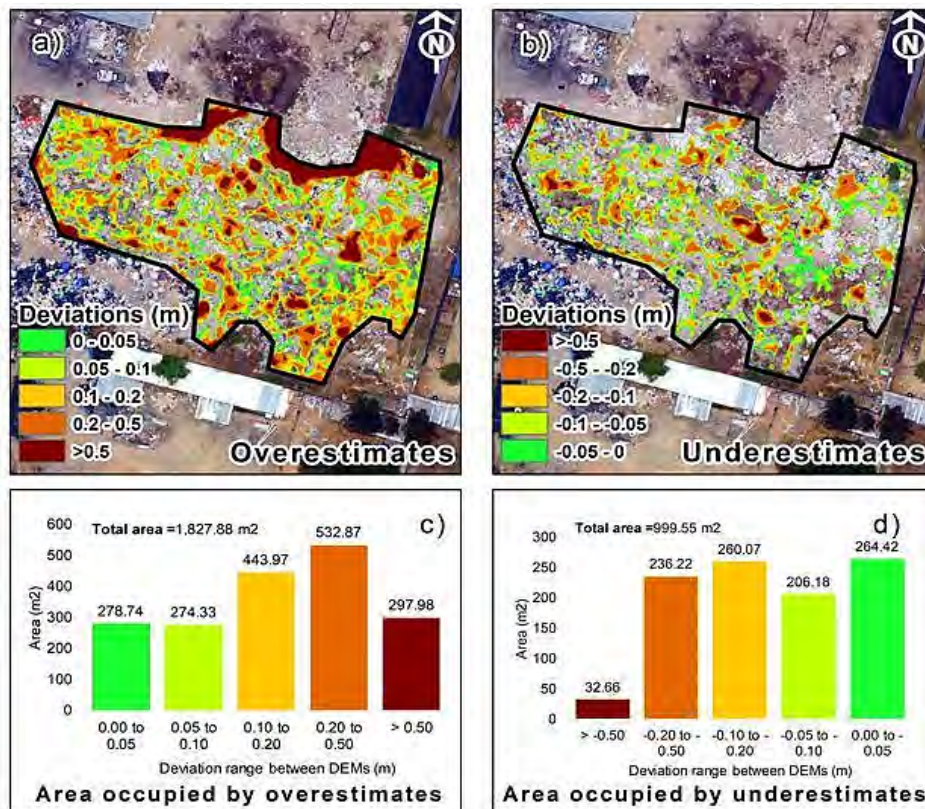

Fig. 4. Differences between DEM built and collected points: a) spatial distribution map of overestimates; b) spatial distribution map of underestimates; c) overestimates in terms of areas; d) underestimates in terms of areas
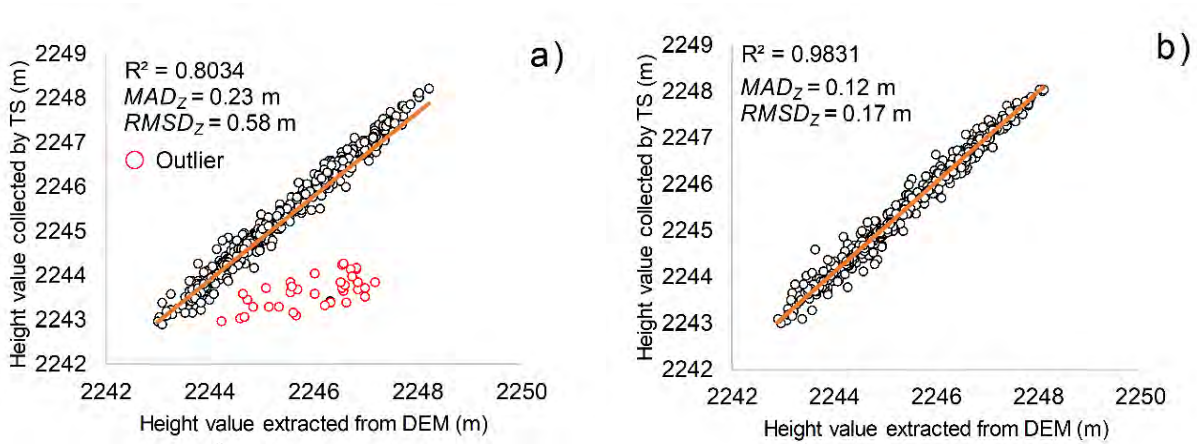
Fig. 5. Analysis of points: a) analysis of the total points collected in the field;
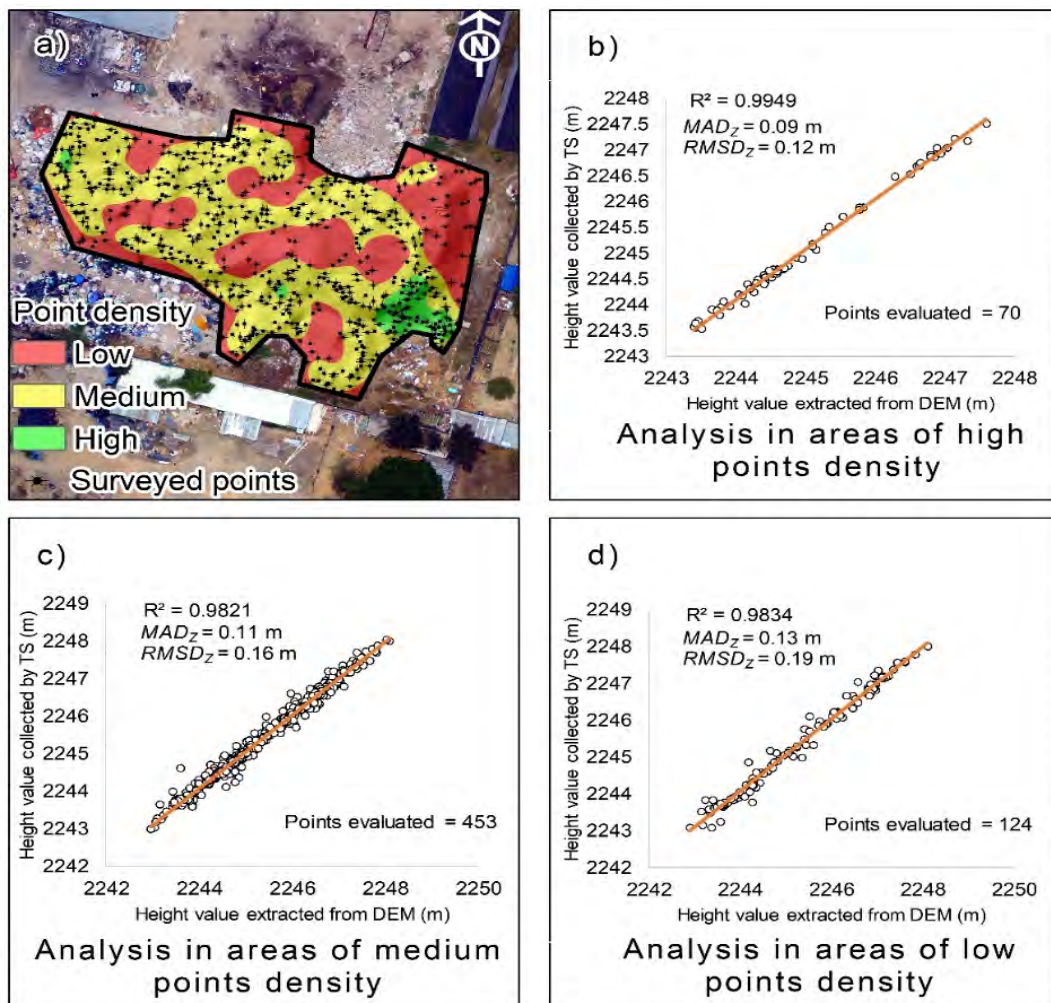b) analysis of points without data with high deviations

Fig. 6. Analysis of zones with different point densities: a) point density map; b) areas with high point density;
c) areas with medium point density; d) areas with low point density

3.2. Analysis of cross sections and volumes

Fig. 7 shows the sections drawn along the length and width of the CDW storage area of both DEMs. The red line represents the section of the surface surveyed with UAVs, while the blue line represents the surface built from TS data. In these cross sections, the greatest differences are located at the extremes, while deviations are smaller in the central areas. Similarly to what is mentioned above, the differences are caused by the low density of points measured by TS, compared to the dense cloud of points obtained from the processing of photogrammetric data.

The largest deviations found on the right side of the Figures are due to external or accidental errors related to the handling of CDW. Note that the survey carried out with UAVs generates a cross section that is more faithful to the real roughness formed by the CDW mounds (more noticeable in Fig. 7a-b), while the surface created by the ET points shows a more stylized flattened cross section (more noticeable in Fig. 7c-d). Table 3 shows the comparison of volumes between both surface DEMs. It is observed that there is a difference of 512 m^3 between them, the volume obtained by the UAV survey being 6.6% greater than the one generated by the TS survey. This volume differential is high, but not unusual. In other studies, such as Hoon et al. (2018), Hugenholtz et al. (2015), Sun et al. (2020), where similar techniques have been applied to survey surfaces and compare volumes generated by photogrammetric work with UAVs and other devices, the differentials range from 1.1 to 3.9%.

For practical purposes, the information generated by the photogrammetric method with UAVs can be considered useful, since this method represents a huge time saving in data collection without a notable loss of precision. Additionally, this method also offers much richer data than the vector data obtained from the TS survey (points, text, and lines), for example, video, aerial photography, and point cloud exportable to other software.

4. Conclusions

In this work, photogrammetry with UAVs was used to quantify CDW temporarily stored in plot of land. The results were compared with those obtained from a classic survey (with TS) through different precision metrics, both for the DEMs generated and for the points obtained. The results of both ways of surveying objects on surfaces indicate that, despite presenting some important deviations, the photogrammetric method with UAVs is usually very useful since it leads to enormous time savings in data collection and offers a large amount of information.

On the other hand, despite generating more accurate results, surveys with TS require too many sampling points, especially in the case of mountainous or rugged terrain with excessive surface irregularities. In fact, in this work the main differences between the DEMs, height values or even volumes, were due to the fact that this survey method had an insufficient density of sampling points within the study area.

Table 3. Comparison of CDW volume by both survey methods

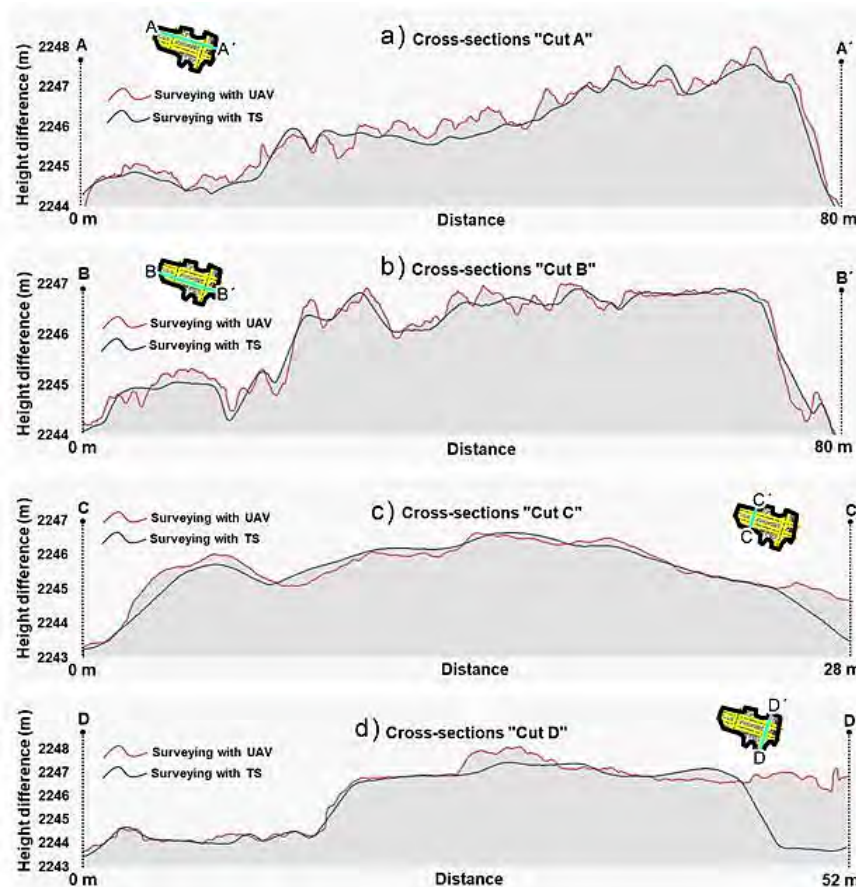| *Volume calculation from Photogrammetric survey with UAVs (m^3)*	*Volume calculation from survey with TS (m^3)*	*Difference (m^3)*
8,199.29	7,686.91	512.38

Fig. 7. Cross sections through the created DEM surfaces

The results generated by this work can be used in decision-making, especially to implement CDW management and control policies. For example, the number of trucks needed to remove improperly stored CDW can be easily quantified from the volume data obtained.

Acknowledgments

References

Agüera F., Carvajal F., Martínez P., (2017), Assessment of photogrammetric mapping accuracy based on variation ground control points number using unmanned aerial vehicle, *Measurement*, **98**, 221-227.

Arseni M., Voiculescu M., Puiu L., Iticescu C., Rosu A., (2019), Testing different interpolation methods based on single beam echosounder river surveying. Case Study: Siret River, *International Journal of Geo-Information*, **8**, 1-21.

Bergonse R., Reise E., (2015), Reconstructing pre-erosion topography using spatial interpolation techniques: A validation-based approach, *Journal of Geographical Sciences*, **25**, 196-210.

Bergsdal H., Bohne R., Brattebo H., (2007), Projection of construction and demolition waste in Norway, *Journal of Industrial Ecology*, **11**, 27-39.

Berie H., Burud I., (2018), Application of unmanned aerial vehicles in earth resources monitoring: focus on evaluating potentials for forest monitoring in Ethiopia, *European Journal of Remote Sensing*, **51**, 326-335.

Blišťan P., Kovanič L., (2012), Geodetic methods for efficient spatial data collection, *Journal of Exploration Geophysics, Remote Sensing and Environment*, **2012**, 1-12.

Burrough P., McDonnell R., (1998), *Principles of Geographical Information Systems*, Oxford University Press, Oxford, 1-333.

Cardoso R., Vasco R., de Brito J., Dhir R., (2015), Use of recycled aggregates from construction and demolition waste in geotechnical applications: A literature review, *Waste Management*, **49**, 131-145.

Casella E., Drechsel J., Winter C., Benninghoff M., Rovere A., (2020), Accuracy of sand beach topography surveying by drones and photogrammetry, *Geo-Marine Letters*, **40**, 255-268.

Chen Y., Zhou Y., (2020), The contents and release behavior of heavy metals in construction and demolition waste used in freeway construction, *Environmental Science and Pollution Research*, **27**, 1078-1086.

Chen Z., Li H., Wong C., (2000), Environmental management of urban construction projects in China, *Journal of Construction Engineering and Management*, **126**, 320-324.

Contreras M., Teixeira S., Lucas M., Lima L., Cardoso D., da Silva G., Gregório G., de Souza A., dos Santos A., (2016), Recycling of construction and demolition waste for producing new construction material (Brazil case-study), *Construction and Building Materials*, **123**, 594-600.

Chow E., Kar B., (2017), *Error and Accuracy Assessment for Fused Data: Remote Sensing and GIS*, In: *Integrating Scale in Remote Sensing and GIS*, Quattrochi D., Wentz E., Lam N., Emerson C. (Eds.), CRC Press, Boca Raton, United States, 125-156.

ESRI, (2020), Topo to raster, On line at: https://desktop.arcgis.com/es/arcmap/10.3/tools/spatial-analyst-toolbox/topo-to-raster.htm.

Federman A., Santana M., Kretz S., Gregg J., Lengies M., Ouimet C., Laliberte J., (2017), UAV photgrammetric workflows: a best practice guideline, *ISPRS - International Archives of the Photogrammetry, Remote Sensing and Spatial Information Sciences*, vol. XLII-2/W5, 237-244.

Gangolells M., Casals M., Gassó S., Forcada N., Roca X., Fuertes A., (2009), A methodology for predicting the severity of environmental impacts related to the construction process of residential buildings, *Building and Environment*, **44**, 558-571.

Haala N., Cramer M., Weimer F., Trittler M., (2011), Performance test on UAV-based photogrammetric data collection, *ISPRS - International Archives of the Photogrammetry, Remote Sensing and Spatial Information Sciences*, vol. XXXVIII-1/C22, 7-12.

Habib M., Alzubi Y., Malkawi A., Awwad M., (2020), Impact of interpolation techniques on the accuracy of large-scale digital elevation model, *Open Geosciences*, **12**, 190-202.

Harwin S., Lucieer A., (2012), Assessing the accuracy of georeferenced point clouds produced via multi-view stereopsis from unmanned aerial vehicle (UAV) imagery, *Remote Sensing*, **4**, 1573-1599.

Hoon S., Kyung H., Hee L., (2018), Earth-volume measurement of small area using low-cost UAV, *Journal of the Korean Society of Surveying, Geodesy, Photogrammetry and Cartography*, **36**, 279-286.

Hugenholtz C., Whitehead K., Brown O., Barchyn T., Moorman B., LeClair A., Riddell K., Hamilton T., (2013), Geomorphological mapping with a small unmanned aircraft system (sUAS): Feature detection and accuracy assessment of a photogrammetrically-derived digital terrain model, *Geomorphology*, **194**, 16-24.

Hugenholtz C., Walker J., Brown O., Myshak S., (2015), Earthwork volumetrics with an unmanned aerial vehicle and softcopy photogrammetry, *Journal of Surveying Engineering*, **141**, 1-5.

Jiménez S., Ojeda W., Ontiveros R., Flores J., Marcial M., Robles B., (2017), Quantification of the error of digital terrain models derived from images acquired with UAV, *Agricultural Engineering and Biosystems*, **9**, 85-100.

Kartam N., Al-Mutairi N., Al-Ghusain I., Al-Humoud J., (2004), Environmental management of construction and demolition waste in Kuwait, *Waste Management*, **24**, 1049-1059.

Kleemann F., Lehner H., Szczypińska A., Lederer J., Fellner J., (2016), Using change detection data to assess amount and composition of demolition waste from buildings in Vienna, *Resources, Conservation and Recycling*, **123**, 37-46.

Kovanič L., Šimčák M., (2014), Stock volumes determining as the basis for the plan of opening, preparation and extraction processing in open stone-pit quarries, *Global Journal of Engineering, Design and Technology*, **3**, 4-8.

Kršák B., Blišťan P., Pauliková A., Puškárová P., Kovanic L., Palková J., Zeliznˇaková V., (2016), Use of low-cost UAV photogrammetry to analyze the accuracy of a

digital elevation model in a case study, *Measurement*, **91**, 276-287.

Lau H., Whyte A., Law P., (2008), Composition and characteristics of construction waste generated by residential housing project, *International*, *Journal of Environmental Research*, **2**, 261-268.

Li Y., Liu C., (2018), Applications of multirotor drone technologies in construction management, *International Journal of Construction Management*, **19**, 401-412.

McBean E., Fortin M., (1993), A forecast model of refuse tonnage with recapture and uncertainty bounds, *Waste Management and Research*, **11**, 373-385.

Mouget A., Lucet G., (2014), Photogrammetric archaeological survey with UAV, *ISPRS - International Archives of the Photogrammetry, Remote Sensing and Spatial Information Sciences*, **II-5**, 251-258.

NAUM, (2017), Methodology for locating final disposal sites for construction and demolition waste using geographic information systems: case study Mexico City - Technical report (in Spanish), National Autonomous University of Mexico - Secretariat of Science, Technology and Innovation. Mexico City, Mexico.

Nex F., Remondino F., (2014), UAV for 3D mapping applications: a review, *Applied Geomatics*, **6**, 1-15.

OGFD, (2015), Environmental Standard for the Federal District NADF-007-RNAT-2013, which establishes the classification and management specifications for construction and demolition wastes, in the Federal District, Official Gazette of the Federal District, On line at: https://www.cmic.org.mx/comisiones/Sectoriales/medi oambiente/PROY-NADF-007-RNAT-2013/ Gaceta_DF_NADF-007-RNAT-2013.pdf.

Otto A., Agatz N., Campbell J., Golden B., Pesch E., (2018), Optimization approaches for civil applications of unmanned aerial vehicles (UAVs) or aerial drones: A survey, *Networks*, **72**, 411-458.

Poon C., Yu A., See S., Cheung E., (2004), Minimizing demolition wastes in Hong Kong public housing projects, *Construction Management and Economics*, **22**, 799-805.

Poon C., (1997), Management and recycling of demolition waste in Hong Kong, *Waste Management and Research*, **15**, 561-572.

Rusnák M., Sládek J., Kidová A., Lehotský M., (2018), Template for high-resolution river landscape mapping using UAV technology, *Measurement*, **115**, 139-151.

Sanz E., Chandler J., Rodríguez J., Ordóñez C., (2018), Accuracy of Unmanned Aerial Vehicle (UAV) and SfM photogrammetry survey as a function of the number and location of ground control points used, *Remote Sensing*, **10**, 1-19.

Sun C., Jae L., Soo L., Hee Y., (2020), A Study on DEM-based automatic calculation of earthwork volume for BIM application, *Journal of the Korean Society of Surveying, Geodesy, Photogrammetry and Cartography*, **38**, 131-140.

Suziedelyte J., Puziene R., Stanionis A., Tumeliene E., (2016), Unmanned aerial vehicles for photogrammetry: analysis of orthophoto images over the territory of Lithuania, *International Journal of Aerospace Engineering*, **2016**, 1-9.

Uysal M., Toprak A., Polat N., (2015), DEM generation with UAV photogrammetry and accuracy analysis in Sahitler hill, *Measurement*, **73**, 539-543.

Wu Z., Yu A., Poon C., (2019), An off-site snapshot methodology for estimating building construction waste composition - a case study of Hong Kong, *Environmental Impact Assessment Review*, **77**, 128-135.

Wu Z., Yu A., Shen L., Liu G., (2014), Quantifying construction and demolition waste: An analytical review, *Waste Management*, **34**, 1683-1692.

Yost P., Halstead J., (1996), Methodology for quantifying the volume of construction waste, *Waste Management and Research*, **14**, 453-461.

Yu D., Duan H., Song Q., Li X., Zhang H., Zhang H., Liu Y., Shen W., Wang J., (2018), Characterizing the environmental impact of metals in construction and demolition waste, *Environmental Science and Pollution Research*, **25**, 13823-13832.

Zolfagharian S., Nourbakhsh M., Irizarry J., Ressang A., Gheisari M., (2012), *Environmental Impacts Assessment on Construction Sites*, Construction Research Congress: Construction Challenges in a Flat World, West Lafayette, Indiana, United States, 1750-1759.